Assembly of *Xenopus* Transcription Factor III A–5S RNA Complex†

Thomas P. Callaci,‡ Guang-Zuan Cai,‡ James C. Lee,*,‡ Thomas J. Daly,§ and Cheng-wen Wu§,‖

E. A. Doisy Department of Biochemistry, St. Louis University School of Medicine, St. Louis, Missouri 63104, and Department of Pharmacological Science, State University of New York at Stony Brook, Stony Brook, New York 11794

Received November 21, 1989; Revised Manuscript Received January 19, 1990

ABSTRACT: The regulation of *Xenopus* 5S rRNA gene expression involves multiple protein factors, among which is transcription factor III A (TFIIIA). This factor can be isolated as a protein–RNA complex. The assembly behavior of this complex was studied by sedimentation velocity and gel electrophoresis at pH 7.5 and 23 °C. The reaction boundary was monitored by the absorbance at 260 nm; thus, the shape of the boundary reflects mainly RNA or RNA-containing complexes. Values for the weight-average sedimentation coefficient ($\bar{s}_{20,w}$) change with protein–RNA concentration. At low concentrations, values of $\bar{s}_{20,w}$ increase with increasing concentration. The extrapolated value for $\bar{s}_{20,w}$ at infinite dilution is 5.2 S, the same value for free *Xenopus* rRNA under the same experimentation conditions. Furthermore, the same value of $\bar{s}_{20,w}$ at a specific RNA concentration can be obtained either by dilution of a concentrated sample or by concentrating a diluted one. These results indicate that complex formation can be described by a reversible process. When the data are analyzed by computer fitting, the *simplest* model that fits the sedimentation data is that TFIIIA and RNA form a 1:1 complex which self-aggregates to a dimer. The sedimentation coefficients ($s^0_{20,w}$) of PR and $(PR)_2$ are 7.5 and 10.6 S, respectively, where PR and $(PR)_2$ are the 1:1 TFIIIA–RNA complex and its dimer, respectively. The protein–RNA interaction was also investigated by gel electrophoresis. The resolved components were identified by differential staining for protein and RNA on a single gel. One band corresponding to free 5S rRNA was detected in addition to two bands which stained for both protein and nucleic acids. The mass ratio of these two protein–RNA complexes was determined to be 2.3, implying that one complex is probably a dimer of the other. These electrophoretic results indicate that at low concentration TFIIIA and RNA exist as individual free entities. At higher concentration, they form a complex which dimerizes. These results are totally consistent with that of sedimentation. In summary, the *Xenopus* TFIIIA–RNA complex undergoes a reversible equilibrium of macromolecular assembly which is characterized as TFIIIA + RNA ⇄ TFIIIA–RNA complex ⇄ (TFIIIA–RNA complex)$_2$.

Developing *Xenopus* oocytes synthesize a large amount of 5S ribosomal RNA (rRNA) which is coded by oocyte and somatic 5S DNA (Federoff & Brown, 1978; Peterson et al., 1980). The 5S rRNA is not immediately assembled into ribosomes but instead is stored as ribonucleoprotein particles (Mairy & Denise, 1971; Thomas, 1969), one of which is the transcription factor III A (TFIIIA)–5S rRNA complex (Picard & Wegnez, 1979; Pelham & Brown, 1980). TFIIIA in conjunction with at least two other protein factors, TFIIIB and TFIIIC, regulates the transcription of 5S rRNA by binding to the internal control region in the 5S DNA [for a review, see Wolff and Brown (1988)]. Hence, regulation of the transcription of 5S ribosomal RNA in *Xenopus* is the consequence of a network of intricately linked reactions involving macromolecular assemblies of protein–protein and protein–nucleic acids.

One of the major issues is to identify the signal or controlling factor(s) that regulate(s) the binding of TFIIIA to 5S rRNA and 5S DNA. A possibility is simply the differences in binding affinities of TFIIIA for 5S rRNA and 5S DNA. This difference in affinity can be amplified by the changing of TFIIIA concentration. At different developmental stages, oocyte or somatic 5S rRNA is differentially synthesized. There is ample evidence to show that both oocyte and somatic 5S RNA genes are transcriptionally active (Brown & Schlissel, 1985; Gergiulo et al., 1984; Wolff et al., 1986). Hence the controlling factors to differentiate between transcribing oocyte and somatic 5S RNA genes must rely on the presence of other factor(s) or fluctuation in the concentration of TFIIIA. Early in oogenesis, there is a large amount of TFIIIA present, but its concentration decreases as oogenesis and embryogenesis progress (Wolff & Brown, 1988); hence, during the various stages of development, the concentration of TFIIIA fluctuates. It is conceivable that the concentrations of other transcription factors may fluctuate too, thus influencing the amount of transcription complexes which in turn may lead to the differentiation of expressing the oocyte or somatic 5S rRNA gene. In order to assess the functional role of fluctuation in the concentration of TFIIIA, it is important to define the mechanism of TFIIIA–nucleic acid interactions. Thus, a systematic study was initiated to investigate the interaction between TFIIIA and 5S rRNA.

Materials and Methods

Purification of Xenopus TFIIIA–5S RNA Complex. The complex was isolated and purified from immature *Xenopus* oocytes by glycerol gradient centrifugation (Pelham & Brown, 1980) and DEAE-cellulose chromatography (Hanas et al., 1983).

Sedimentation Velocity. Experiments were conducted in Hepes buffer (20 mM Hepes, 1.5 mM $MgCl_2$, 50 mM KCl, and 0.5 mM DTT at pH 7.5) with a Beckman Model E

† Supported by NIH Grants NS-14269, DK-21489, and GM-11058 (J.C.L.) and by NIH Grant GM-28069, NSF Grant 800313, and ACS Grant CD-306 (C.W.).

* Author to whom correspondence should be addressed.

‡ St. Louis University School of Medicine.

§ State University of New York at Stony Brook.

‖ Present address: Institute of Biomedical Sciences, Academia Sinica, Taipei, Taiwan 10529, Republic of China.

0006-2960/90/0429-4653$02.50/0

analytical ultracentrifuge equipped with an ultraviolet scanner, electronic speed control, and RTIC temperature control. Double-sector, aluminum-filled or charcoal-filled Epon centerpieces, and sapphire windows were used in AN-D or AN-E rotors at 60000 and 52000 rpm, respectively. The UV scanner was used to trace the reaction boundary during sedimentation at 260 nm. At this wavelength, the molar absorptivity of RNA is approximately 17 times that of protein. Hence, the contribution of absorption by protein to the reaction boundary can be approximated as zero.

Weight-average sedimentation coefficients, $\bar{s}$, were determined from the centroid, a close approximation of the second moment, of the scanner-traced boundaries in a manner analogous to that of Arisaka and Van Holde (1979). The observed $\bar{s}$ values were normalized to standard conditions by correcting for solvent density and viscosity.

For an associating system, $\bar{s} = \sum_i s_i C_i / \sum C_i$ where s_i and C_i are the sedimentation coefficients and concentrations of the ith species, respectively (Schachman, 1959). In expressing each sedimentation coefficient, s_i, as a function of the total concentration of TFIIIA–5S RNA complex, C, then

$$\bar{s} = \sum_i s^0_i (1 - g_i C) K_i C_1^i / \sum_i K_i C_1^i \qquad (1)$$

where s_i^0 is the sedimentation coefficient of the ith species at infinite dilution, g_i is the nonideality coefficient, $C = \sum_i K_i C_1^i$, K_i is the equilibrium constant between any i-mer and the monomer, and C_1 is the monomer concentration.

Theoretical values of $\bar{s}$ as a function of C_1, s_i^0, g_i, and K_i can be fitted to the observed weight-average sedimentation coefficients as a function of C; thus, the best-fit curve can yield information on the physical parameters which govern the assembly process of the TFIIIA–5S RNA complex.

Native Polyacrylamide Gel Electrophoresis. Native PAGE experiments were conducted in a Bio-Rad Mini Protean II gel apparatus with the same Hepes buffer as that in sedimentation studies. Routinely, a 6% acrylamide [29:1 acrylamide:bis(acrylamide) ratio] gel was employed, and the electrophoresis was conducted at 15–20 mA, 40 V, for 2 h. It was found that under these conditions optimum results can be obtained.

The study was conducted as a function of complex concentration; however, the amount of complex loaded in each lane was kept constant. Volumes of 5–25 μL of samples were loaded on each lane. Marker dye (Bromophenol Blue and Xylene cyanol in 30% glycerol) was found to affect the protein–RNA complex and was not added to the sample lanes. In all circumstances, glycerol was added to the samples to a final concentration of 3% to aid in loading.

Staining Procedures. A selective silver staining procedure was employed to distinctively stain for protein and RNA (Paleologue et al., 1988). The first step of this method allowed detection of free RNA or RNA-containing complex as brown bands. The second step allowed detection of free protein or protein-containing complex as a purple band with increase in the coloration of the protein–RNA bands. The specifics of the procedure are as follows:

(*I*) *Nucleic Acid Staining.* Gels were covered by a solution of methanol/acetic acid/water (50:7.5:42.5 v/v/v) with gentle agitation in a sealed container overnight. The solution was replaced by another one of 3.4 mM $K_2Cr_2O_7$ and 3.2 mM HNO_3 with gentle agitation for 6 min, after which the gels were washed with deionized–distilled water 3 times, 10-s duration for each wash. The gels were stained by a 20 mM $AgNO_3$ solution with a 3-min exposure to short-wavelength UV light while agitating by hand. After the gels were washed with deionized–distilled water for 20 s, the coloration of the stained gels was developed by rapid rinsing of the gels 2 times with 200–300 mL of a developing solution (280 mM Na_2CO_3/0.0037% HCHO) and then 1 or 2 times for 5–15 min until the desired intensity was reached. The color development was arrested by exposure to a 1% solution of acetic acid and subsequently washed with deionized–distilled water.

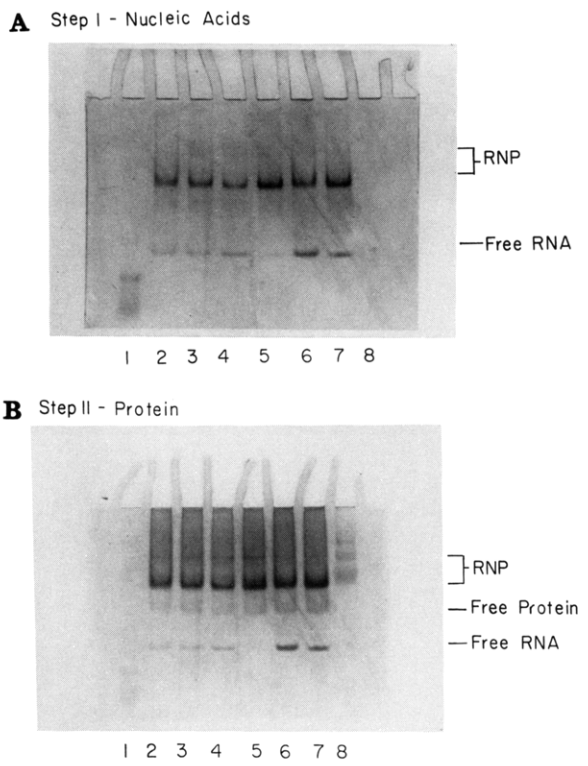

FIGURE 1: Native gel electrophoresis study of the TFIIIA–5S rRNA particle at pH 7.5, 23 °C. Electrophoretic patterns as a function of particle concentration ranging from 6 to 18 μg/mL. tRNA and BSA were used as standards for nucleic acid and protein in the first and last lanes, respectively. The amount of particle was kept constant in each lane. (A) Stained for nucleic acids; (B) stained for protein.

(*II*) *Protein Staining.* The gels were soaked in a 10% solution of glutaraldehyde for 30 min with gentle agitation. After the gels were rinsed 3 times with deionized–distilled water, the gels were immersed in a 10% solution of EtOH with agitation 4 times for 20 min each. The gels were stained with a solution of 20 mM $AgNO_3$, 20 mM NaOH, and 0.25% NH_4OH for 15 min with moderate agitation. After the gels were rinsed with deionized–distilled water, the coloration of the gels was developed by a solution of 0.26 mM citric acid/1.3% HCHO. The development of coloration was stopped by rinsing the gels with a 1% solution of acetic acid, after which the gels were destained with Kodak Rapid Fix solution. Destaining was stopped with Kodak hypo cleaning agent at 1:1 dilution.

Results

To elucidate the mechanism of complex formation between TFIIIA and 5S RNA and to determine the impact of the fluctuation in TFIIIA concentration on the reaction(s), the purified TFIIIA–RNA complex was subjected to electrophoretic analysis at pH 7.5 and 23 °C as a function of particle concentration ranging from 6 to 48 μg/mL. The gels were stained selectively for protein and nucleic acids by the silver staining procedure of Paleologue et al. (1988). Typical results of such a study are shown in Figure 1A,B. After the first step of selective staining for RNA, three distinct bands were observed, as shown in Figure 1A. One band, which corresponds to that of free 5S RNA, is the predominant one at low

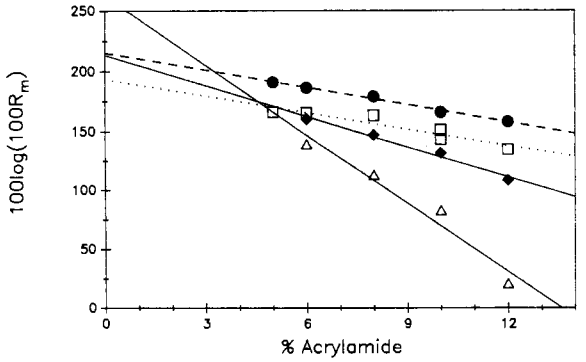

FIGURE 2: Relative electrophoretic mobilities of protein–nucleic acid complexes as a function of acrylamide percentage. Symbols and identities of complex with respect to electrophoretic mobility are (△) slow moving and (♦) fast moving. (□) and (●) are free protein and RNA, respectively. R_m is the ratio of the distance migrated by the particle with respect to that of Bromophenol blue.

concentration. With increasing concentration, a second band and a third band with slower mobilities appear. The appearance of the bands with slower electrophoretic mobility is concentration-dependent, implying that these three bands represent products of an association–dissociation equilibrium. It is important to note the selectivity of this staining step for nucleic acids. Only the control lane with tRNA is stained whereas the control lane with BSA is clear. Thus, all of the bands observed at this point only represent those containing RNA. After selectively staining for protein on the same gel, two distinct bands are observed, as shown in Figure 1B. These bands correspond to two of the RNA bands shown in Figure 1A. One may conclude that these two bands represent protein–RNA complexes. Again, the selectiveness of the staining procedure for protein was demonstrated by the staining of the BSA-containing control lane. Combination of both staining steps enhances the staining for nucleic acids; thus, bands corresponding to the protein–RNA complexes can be observed even at the lowest concentration. In order to assess the ratio of the masses of these two protein–RNA complexes, electrophoretic mobilities of these bands were monitored as a function of acrylamide concentration in a procedure analogous to that described for protein (Hedrick & Smith, 1968). Results of this study are summarized in Figure 2. The slopes of the plots of log mobility vs percent acrylamide should be proportional to the mass of these components (Hedrick & Smith, 1968). The calculated slopes of these two protein–RNA bands are −8.5 and −19.3, which yield a ratio of 2.3, a value implying that the mass of one complex is twice that of the other, e.g., dimer and monomer of a protein–RNA complex. It is interesting to note that the slopes of free RNA and protein are essentially identical although the intercepts are different. These results are totally consistent with the fact that TFIIIA and 5S RNA assume essentially identical mass but with different net charges.

The simplest conclusion of the electrophoretic results is that the TFIIIA–RNA complex undergoes reversible association–dissociation. At a low concentration of 6 μg/mL, some of the complex dissociated into its constituents of TFIIIA and 5S RNA. With increasing concentrations, TFIIIA and 5S RNA form a complex which further dimerizes. To demonstrate that these bands are products of a reaction in equilibrium, the relative concentrations of one band to another, as monitored by densitometric scanning, are expressed as total TFIIIA–RNA complex concentration. The ratio of free RNA to the monomeric protein–RNA complex decreases with increasing concentrations whereas that for the dimer to monomer in-

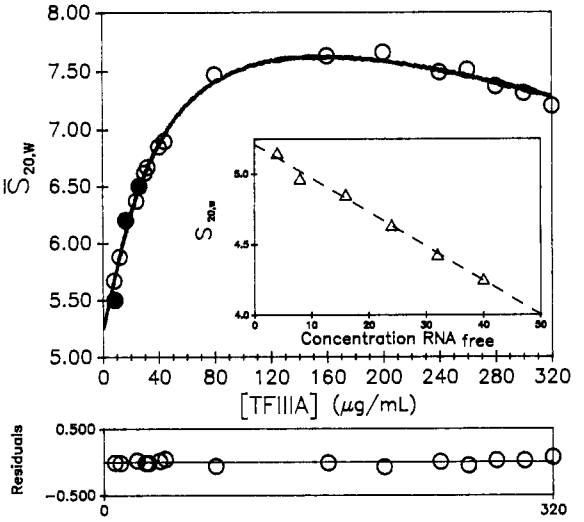

FIGURE 3: Relation between the weight-average sedimentation coefficient and TFIIIA–RNA complex concentration in Hepes buffer at pH 7.5 and 23 °C. The sedimentation of the RNA was monitored by setting the monochromator at 260 nm. Symbols and sample history are (○) purified RNA–protein complex and (●) RNA–protein complex that was diluted from a stock solution and then reconcentrated by filtration through a Centricon filter; (△) free RNA. The solid line is the best fit according to the reaction scheme of eq 2.

creases with increasing concentrations. These results support the interpretation that these components are in equilibrium. Hence, the electrophoretic results are consistent with an assembly process described as

$$R + P \overset{K_0}{\rightleftharpoons} RP \overset{K_i}{\rightleftharpoons} (RP)_i \qquad (2)$$

where R and P represent 5S RNA and TFIIIA, respectively, $i = 2$, and K_i is the corresponding equilibrium constant of these reactions.

The electrophoretic approach is not precise enough to permit a quantitative evaluation of the assembly properties of TFIIIA and 5S RNA. Furthermore, the values of equilibrium constants estimated by this electrophoretic method may not be accurate (Cann, 1989). In order to provide an independent measurement of the assembly process and quantitatively assess the effect of fluctuation in TFIIIA concentration, sedimentation analysis was conducted at pH 7.5 and 23 °C. The scanner was set at 260 nm to monitor the reaction boundary. Since the absorption of TFIIIA at 260 nm at an equivalent concentration is only 6% of 5S RNA, the sedimentation profiles are significantly simplified. The sedimentation profile of the RNA is monitored while the protein is essentially transparent under these conditions. No bimodality was observed in the sedimentation boundary during this study. This observation implies that the TFIIIA–5S RNA complex does not undergo a cooperative association–dissociation reaction that is characterized by a stoichiometry of 3 or greater (Gilbert, 1955, 1959, 1963). However, the values of $\bar{s}$ are a function of particle concentration, as shown in Figure 3. The values of $\bar{s}$ increase initially with increasing concentration, indicating that the system undergoes association–dissociation. At approximately 100 μg/mL, the $\bar{s}$ values level off and subsequently decrease. The leveling off and decrease in $\bar{s}$ value at high concentration are the consequence of hydrodynamic nonideality (Schachman, 1959). Before the data can be analyzed for mode of association and equilibrium constants, it is essential to demonstrate that the results actually reflect the product of a reversible equilibrium or coupled equilibria; hence, a solution of particle at 26 μg/mL was subjected to sedi-

mentation analysis. The same sample was diluted to 7 μg/mL and subsequently reconcentrated to 17 μg/mL. Both the diluted and reconcentrated samples were subjected to sedimentation analysis, and the results are shown as solid circles in Figure 3. It is evident that the $\bar{s}$ values of these samples fit into the same curve of $\bar{s}$ vs concentration; thus, these results strongly support the notion that this study is indeed monitoring the equilibrium distribution of species of a reversible reaction.

At infinite dilution, the extrapolated $\bar{s}$ value of 5.2 S was observed. In order to establish the identity of the 5.2S component, the 5S RNA was purified from *Xenopus* oocyte by electrophoresis in an acrylamide/urea gel (Birkenmeyer et al., 1978) and then subjected to sedimentation analysis under the same experimental conditions as those of the particles. The results are shown in Figure 3. It is evident that purified 5S RNA sedimented as a single component without any propensity to undergo any association–dissociation reaction. A linear extrapolation of $\bar{s}$ vs concentration was observed, yielding a value of 5.2 S for $s^0_{20,w}$ for the 5S RNA. Hence, the sedimentation data of the TFIIIA–RNA complex indicate that at low concentrations, the complex dissociates into free 5S RNA. From these sedimentation studies, it may be concluded that the TFIIIA–5S RNA complex undergoes rapid reversible association. The smallest species participating in the reaction is most likely the free 5S RNA and TFIIIA.

In order to determine the physical constants characteristic of this association–dissociation reaction, a quantitative analysis was initiated by theoretical fitting of the concentration dependence of the weight-average sedimentation coefficient by means of a nonlinear least-squares method (Marquardt, 1963), a procedure routinely employed by one of the laboratories in the study on self-association of rabbit muscle phosphofructokinase (Hesterberg & Lee, 1981, 1982; Luther et al., 1986). The procedure requires good initial estimates of the parameters s^0_i, g_i, and K_i. Refinement of these values is accomplished by a reiteration scheme using the root mean square deviation as a criterion of convergence. Since the reaction under investigation includes the protein–RNA complex and its dissociation products, eq 1 was modified to simplify the procedure for analysis. The modified eq 1 is expressed as

$$\bar{s} = \{s^0_R(1 - g_R C)(C_{RP}/K_0)^{1/2} + \sum_i s^0_{(RP)_i}[1 - g_{(RP)_i} C]K_i C^i_{RP}\}/\sum_i K_i C^i_{RP} \quad (1a)$$

where s^0_R and $s^0_{(RP)_i}$ are sedimentation coefficients of 5S RNA and TFIIIA–RNA complexes of different sizes with $i = 1, 2, 3, \ldots$, respectively, g_R and $g_{(RP)_i}$ are the corresponding hydrodynamic nonideality parameters for 5S RNA and TFIIIA–RNA complexes, respectively, and C_{RP} and C are the concentrations of the monomeric 1:1 TFIIIA–RNA complex and total RNA, respectively. The value of g_R was estimated from the slope of $s_{20,w}$ vs C for rRNA (inset of Figure 3) while the value of $g_{(RP)_i}$ was from the plot for a high concentration of TFIIIA–RNA complex in Figure 3. Values of 0.005 mL/μg and 4.4×10^{-4} mL/μg were determined for g_R and $g_{(RP)_i}$ respectively. It is assumed that all oligomeric forms of TFIIIA–RNA complex exhibit the same nonideality behavior which is significantly different from that of free RNA. The value for $g_{(RP)_i}$ represents a minimum, since it represents the composite of two opposing factors, namely, self-association and nonideality. The uncertainty for $g_{(RP)_i}$ does not affect the association constants significantly.

The intrinsic sedimentation coefficient of RNA is 5.2 S, whereas the corresponding values of TFIIIA–RNA complex and the ith species of the complex are not known and are parameters to be fitted. The relationship between the TFIIIA–RNA complex and the ith species of the complex is initially estimated by eq 3. This relationship assumes an

$$s^0_{(RP)_i} = s^0_{RP}(i)^{2/3} \quad (3)$$

identical frictional ratio of all species (Cann, 1970; Nichol et al., 1964); however, subsequently the values for $s^0_{(RP)_i}$ are variables to be fitted.

Table I: Summary of Fitting for Weight-Average Sedimentation Velocity Data at pH 7.5, 23 °C

model: $R + P \overset{K_0}{\rightleftharpoons} RP \overset{K_i}{\rightleftharpoons} (RP)_i \overset{K_n}{\rightleftharpoons} (RP)_n$

i	n	K_0[a]	K_i	K_n	ss[b]
2	0	0.047	0.067		0.088
2	3	0.053	0.068	7.9×10^{-6}	0.104
2	4	0.051	0.069	1.3×10^{-8}	0.118
3	0	0.067	1.726		1.726
4	0	0.031	7.5×10^{-6}		6.256

[a] Solute concentration expressed in units of milliliters per microgram. [b] Sum of the squares of residuals.

Knowing the basic assumptions, the fitting procedure was employed to estimate the mode of association and the equilibrium constants involved in the reaction scheme of TFIIIA–RNA at pH 7.5 and 23 °C. The *simplest* model that is consistent with the sedimentation data is identical with that deduced from the electrophoretic results as expressed by eq 2, namely, at low concentration, TFIIIA–RNA complex dissociates into its constituent components of TFIIIA and RNA, and also the complex dimerizes at high concentrations. The parameters that fit the results best are summarized in Table I, and the calculated $\bar{s}$ vs concentration curve is shown in Figure 3. It is evident that the fit is good with random distribution of residuals. The values of s_{RP} and $s_{(RP)_2}$ are deduced to be 7.5 and 10.6 S, respectively. The sedimentation results were also fitted to other models, e.g., trimerization and tetramerization of the RP complex. Table I shows that the sum of the squares of residuals (ss) for those models are significantly higher than that of dimerization of RP. Results of F test show that to achieve a 95% level of confidence to reject these models, the values of ss should be >0.23. For the models with $n = 3$ or 4, the values of ss are significantly greater than 0.23, so these models can be rejected with 95% confidence. The models for sequential polymerization of the RP complex have also been tested. Based strictly on the values of ss, it is not possible to rule out these models. However, the values for the association constants are vanishingly small; thus, the presence of these oligomeric specifies is insignificant. Therefore, it can be concluded that the sedimentation data are consistent with the model as shown in eq 2. The association constant, k_i, in units of M^{-1} is related to K_i by $k_i = K_i M_1/2$, where K_i is in units of liters per gram and M_1 is the molecular weight of the associating unit. Thus, for calculating k_0 and k_2, M_1 assumes the value for the molecular weight of rRNA or TFIIIA and TFIIIA–rRNA complex, respectively. rRNA and TFIIIA essentially are of the same molecular weight of 38 500; thus, the molecular weight of the 1:1 complex is assumed to be 77 000. The values of k_0 and k_2 are 0.9×10^6 and 2.6×10^6 M^{-1}, respectively.

Changing the stoichiometry of the second step in eq 2 by setting $i = 0$, 3, or 4 yielded ss values >1. Thus, the sedimentation results are not consistent with these models. These fitting results are in total agreement with the experimental observation that at no concentrations was biomodality apparent in the reacting boundary, a diagnostic phenomenon for a cooperative association with a stoichiometry of ≥3 in accordance to the Gilbert theory (Gilbert, 1955).

Table II: Summary of Fitting for Sedimentation Coefficients for RP and $(RP)_2$ Complexes

s_1[a]	s_2	ss	s_1[a]	s_2	ss
6.3	10.0	0.4947	7.2	11.4	0.6464
	10.5	0.1675		10.6	0.1203
6.5	10.3	0.1978	7.3	11.6	0.7578
	10.5	0.1523		10.5	0.1132
6.7	10.6	0.1488	7.4	11.8	0.8972
	10.5	0.1368		10.6	0.1063
6.9	11.0	0.3832	7.5	11.9	0.8751
	10.5	0.1428		10.6	0.0878
7.0	11.1	0.4222	7.6	12.1	1.0480
	10.6	0.1240		10.6	0.0950
7.1	11.3	0.5900	7.7	12.2	1.061
	10.5	0.1056		10.6	0.0950

[a] s_1 and s_2 are sedimentation coefficients for RP and $(RP)_2$ complexes, respectively. With each fixed value of s_1, the fitting procedure is initiated with s_2 as a fitting parameter, and the corresponding ss value is generated. The first value of s_2 for each corresponding s_1 is calculated in accordance to eq 3, whereas the second value of s_2 represents the best fitting with the fixed s_1 value.

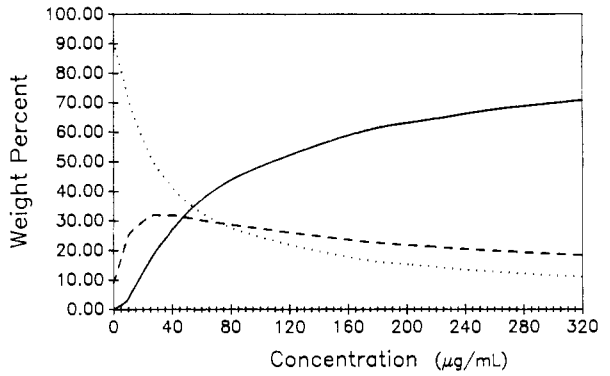

FIGURE 4: Calculated mass distribution of free RNA and monomeric and dimeric TFIIIA–RNA complex as a function of complex concentration. Symbols and identities of species are (···) free RNA, (---) monomeric TFIIIA–RNA complex, and (—) dimeric TFIIIA–RNA complex.

In order to demonstrate that these s values do represent the best estimates under these experimental conditions, the s values for RP and $(RP)_2$ were systematically changed. The pair of s values that yields the smallest ss values are 7.5 and 10.6. With any deviations from 7.5 and 10.6 S, the sum of squares of residuals increases, indicating the poorness of fit, as summarized in Table II. Under all circumstances, the pairs estimated by eq 3 yield significantly higher ss values; thus, it appears that this relationship may not hold for this system. The value of s^0_{RP} at a 75% level of confidence ranges from 6.9 to 9.5 S, whereas the corresponding value for $s^0_{(RP)_2}$ at a 95% level of confidence ranges from 10.4 to 10.8 S. Even with the relatively high degree of uncertainties in the value for s^0_{RP}, the association constants only vary from 0.4×10^6 to 1.2×10^6 M^{-1} for k_0 and from 1.8×10^6 to 2.8×10^6 M^{-1} for k_2.

Figure 4 depicts the calculated mass distribution of different species as a function of total TFIIIA–RNA complex concentration based on the best-fit parameters. The distribution was calculated in terms of the association mechanism described in eq 2 at pH 7.5 and 23 °C. The weight percentage of free 5S RNA decreases with increasing complex concentration. The monomeric 1:1 TFIIIA–RNA complex increases to a maximum of 32% at 31 μg/mL complex and decreases slowly with increasing concentration. This decrease in the monomeric complex is accompanied by an increase in the dimeric form of the 1:1 TFIIIA–RNA complex. These observations are in good agreement with qualitative analysis of the electrophoretic data.

Discussion

One of the most intriguing properties concerning TFIIIA is its ability to bind to both RNA and DNA. Many studies were conducted to investigate the specificity of TFIIIA with respect to the source of RNA (Hanas et al., 1984; Sands & Bogenhagen, 1987; Romaniuk, 1985) and single/double-strand DNA [see Hanas et al. (1984), Windsor et al. (1988), and Wolffe and Brown (1988) for a review] and the structural importance of RNA (Romanick et al., 1987; Christiansen et al., 1987; Baudin & Romaniuk, 1989). In essentially all cases, TFIIIA was purified by various methods which may lead to denaturation (Smith et al., 1984; Bieker & Roeder, 1984) or residual RNA fragments (Hanas et al., 1983) or low yield (Romaniuk, 1985). The present study obviates these concerns, since the protein–RNA complex is the subject of investigation. The results of this study show not only that TFIIIA undergoes a reverisble association–dissociation with 5S RNA to form a 1:1 protein–RNA complex but also that the complex itself undergoes dimerization. The formation of a dimeric form of the TFIIIA–RNA complex has not been reported before, although as early as 1979, Picard and Wegnez reported an initial observation concerning the change of sedimentation coefficient of the complex as a function of complex concentration. At present, the electrophoretic and sedimentation data unequivocally demonstrate the propensity of the complex to dimerize under the experimental conditions.

The association constant for the formation of protein–RNA complex is $(0.9 \pm 0.4) \times 10^6$ M^{-1}, which is orders of magnitude lower than the values of 1.4×10^9 and 5×10^7 M^{-1} reported by Romaniuk (1985) and Hanas et al. (1984), respectively. The causes of discrepancy are most likely the methods employed in monitoring complex formation and the failure to consider the dimerization of the complex. Let us examine the reason by using the constants determined in this study. The apparent association constant for the reaction shown in eq 2 is

$$k_{app} = k_0(1 + 2k_0k_2[R][P]) \quad (4)$$

Since k_0 and k_2 assume values of 0.9×10^6 and 2.6×10^6 M^{-1}, respectively, then it can be shown that if the concentrations of R and P are in micromolar the value of k_{app} will be significantly higher than k_0, the intrinsic binding constants; e.g., at equal concentrations for R and P of 5 μM, k_{app} would be 118-fold of k_0. Thus, the discrepancy between this study and the literature can be attributed to a failure to consider oligomerization as a coupled reaction to protein–RNA complex formation or employing techniques that perturb the various equilibria in the reaction, e.g., filter binding. If this explanation is valid, then how would this affect the significance of the comparative association constants for various RNAs and DNAs? It is impossible to assess this question at present. It may depend on the coupling of the formation of complex to oligomerization of the complex. As shown by eq 4, k_{app} may reflect the magnitude of k_0 or a complex function, the magnitude of which depends on k_2. Thus, it is imperative that the studies of TFIIIA interacting with DNA and RNA be conducted with cognizance of these coupled reactions.

A careful comparison of the sedimentation and electrophoretic results reveals that the sedimentation data show unimodality throughout the concentration range employed; however, the electrophoretic patterns consistently indicate a clear resolution of the oligomeric species. These results imply that the protein–nucleic acid assembly processes are kinetically controlled. The intrinsic rates of reaching equilibrium are rapid in comparison with the rate of separation of these com-

plexes in the sedimentation experiment, whereas these are slow with respect to electrophoresis. However, the duration of both experiments is similar, e.g., 1–2 h, therefore, the possible difference in the rates of transport is unlikely to be totally responsible for the differences in the results. Another possibility is that the factor(s) specifically associated with gel electrophoresis has (have) altered the rates of reaching equilibrium. One potential factor is the cage effect as discussed by Cann (1989). Because of the restriction of the gel network, the degree of freedom to diffuse and the reaction order are reduced in comparison to that in free solution. Under these specific conditions, complex formation is stabilized, and resolution of components is observed. If the cage effect plays a role, then one may expect that it becomes more difficult to resolve these complexes in low-percentage acrylamide gels when the effective pore sizes are larger. In this study, it is clear from the results shown in Figure 2 that it would be very difficult to resolve these various species at 5% acrylamide. Hence, it may be concluded that the apparent discrepancy between the electrophoretic and sedimentation results is most likely the consequence of the peculiar effect of gel in the thermodynamic behavior of macromolecular complexes, resulting in an appearance of the equilibrium being slow with respect to the time of electrophoresis but fast with that of sedimentation, a process that does not significantly perturb the intrinsic thermodynamic behavior of the TFIIIA–RNA interaction.

Since the sedimentation approach as employed in this study represents the first application to a heterologous system, it is appropriate to discuss the advantages and disadvantages of the approach. Other sedimentation velocity approaches have been introduced in the studies of protein–nucleic acid interactions (Jensen & von Hippel, 1977; Revzin & von Hippel, 1977). These approaches determine the concentrations of nucleic acids and proteins at any time during the centrifugation experiment by taking advantage of the fact that protein and nucleic acid have different absorptivity at different wavelengths. The free and nucleic acid bound protein would sediment at different rates; then, the concentrations of free and bound protein can be determined. This approach requires accurate measurement of concentrations, i.e., absorbance, during the experiment. In this present approach, the accuracy of absorbance is not the primary concern. The key factor is the accuracy in determining the boundary position and in turn the weight-average sedimentation coefficient, $\bar{s}$. The accuracy of determining $\bar{s}$ is enhanced by the fact that it is proportional to the slope of a plot of log radial distance of the boundary versus time; thus, the uncertainties in the boundary measurement are minimized.

The shape of the $\bar{s}$ vs C relation is a function of the reaction mechanism; thus, it contains information of both stoichiometry and equilibrium constants. For example, if one tries to fit the curve shown in Figure 3 without considering dissociation of the TFIIIA–RNA complex, no combinations of s_i, K_i, and g_i can provide a satisfactory fit to the data. Another point of interest is that the observed value of $\bar{s}$ never reached the value of 10.6 S, the deduced value of $s^0_{20,w}$ for the dimer of TFIIIA–RNA complex. One may observe values of $\bar{s}$ to approach 10 S if K_2 is stronger (Gilbert & Gilbert, 1973). Furthermore, the fact that the reaction mechanism is in good agreement with the electrophoretic results indicates the resolving power of this approach. At present, the limitations of this approach in studying associating systems of heterologous components have not been defined. Further studies are in progress to determine the limits of K, the size and concentration of nucleic acids, etc. that can be studied with this approach. Furthermore, one may decide to relax the restriction of monitoring chiefly the behavior of RNA and RNA-containing complexes in order to provide additional information on the free/bound protein also. One may then proceed to analyze this much more complicated boundary by the theory derived by Gilbert and Jenkins (1956, 1959).

In summary, sedimentation and electrophoretic data show not only that the *Xenopus* TFIIIA–RNA complex undergoes dissociation to its macromolecular components but also that the complex can form dimers at higher concentration. Since these reactions are thermodynamically linked, any proposed mechanism of regulation of the transcription of 5S rRNA in *Xenopus* must consider the propensity of oligomerization by the complex or other TFIIIA–nucleic acid complexes.

Acknowledgments

We thank Drs. Brenowitz, Na, and Heyduk for critical reviews of the manuscript.

References

Arisaka, F., & Van Holde, K. E. (1979) *J. Mol. Biol. 134*, 41–73.

Baudin, F., & Romaniuk, P. J. (1989) *Nucleic Acids Res. 17*, 2043–2056.

Bieker, J. J., & Roeder, R. G. (1984) *J. Biol. Chem. 259*, 6158–6164.

Birkenmeyer, E. H., Brown, D. D., & Jordan, E. (1978) *Cell 15*, 1077–1086.

Brown, D. D., & Schlissel, M. S. (1985) *Cell 42*, 759–767.

Cann, J. R. (1970) *Interacting Macromolecules: Theory and Practice of Their Electrophoresis, Ultracentrifugation and Chromatography*, Academic Press, New York.

Cann, J. R. (1989) *J. Biol. Chem. 264*, 17032–17040.

Christiansen, J., Brown, R. S., Sproat, B. S., & Garrett, R. A. (1987) *EMBO J. 6*, 453–460.

Fedoroff, N. V., & Brown, D. D. (1978) *Cell 13*, 701–716.

Gargiulo, G., Razvi, F., & Worcel, A. (1984) *Cell 38*, 511–521.

Gilbert, G. A. (1955) *Discuss. Faraday Soc. 20*, 68–71.

Gilbert, G. A. (1959) *Proc. R. Soc. London, A 250*, 377–388.

Gilbert, G. A. (1963) *Proc. R. Soc. London, A 276*, 354–366.

Gilbert, G. A., & Jenkins, R. C. L1. (1956) *Nature 177*, 853.

Gilbert, G. A., & Jenkins, R. C. L1. (1959) *Proc. R. Soc. London, A 253*, 420–437.

Gilbert, L. M., & Gilbert, G. A. (1973) *Methods Enzymol. 27*, 273–295.

Hanas, J. S., Bogenhagen, D. F., & Wu, C.-W. (1983) *Proc. Natl. Acad. Sci. U.S.A. 80*, 2142–2145.

Hanas, J. S., Bogenhagen, D. F., & Wu, C.-W. (1984) *Nucleic Acids Res. 12*, 2745–2758.

Hedrick, J., & Smith, A. (1968) *Arch. Biochem. Biophys. 126*, 155–164.

Hesterberg, L. K., & Lee, J. C. (1981) *Biochemistry 20*, 2974–2980.

Hesterberg, L. K., & Lee, J. C. (1982) *Biochemistry 21*, 216–222.

Jensen, D. E., & von Hippel, P. H. (1977) *Anal. Biochem. 80*, 267–281.

Luther, M. A., Cai, G. Z., & Lee, J. C. (1986) *Biochemistry 25*, 7931–7937.

Mairy, M., & Denise, H. (1971) *Dev. Biol. 24*, 143–165.

Marquardt, D. W. (1963) *J. Soc. Ind. Appl. Math. 11*, 431.

Nichol, L. W., Bethune, J. L., Kegeles, G., & Hess, E. L. (1964) *Proteins (2nd Ed.) 2*, 305–403.

Paleologue, A., Rebound, J. P., & Rebound, A. M. (1988)

Anal. Biochem. 169, 234–238.
Pelham, H. R. B., & Brown, D. D. (1980) *Proc. Natl. Acad. Sci. U.S.A. 77*, 4170–4174.
Peterson, R. C., Doering, J. C., & Brown, D. D. (1980) *Cell 20*, 131–141.
Picard, B., & Wegnez, M. (1979) *Proc. Natl. Acad. Sci. U.S.A. 76*, 241–245.
Revzin, A., & von Hippel, P. H. (1977) *Biochemistry 16*, 4769–4776.
Romaniuk, P. J. (1985) *Nucleic Acids Res. 13*, 5369–5387.
Romaniuk, P. J., de Stevenson, I. L., & Wong, A. H.-H. (1987) *Nucleic Acids Res. 15*, 2737–2755.
Sands, M. S., & Bogenhager, D. F. (1987) *Mol. Cell. Biol. 7*, 3985–3993.
Schachman, H. K. (1959) *Ultracentrifugation in Biochemistry*, Academic Press, New York.
Smith, D. R., Jackson, I. J., & Brown, D. D. (1984) *Cell 37*, 645–652.
Thomas, C. (1969) *Arch. Int. Physiol. Biochem. 77*, 402–403.
Windsor, W. T., Lee, T.-C., Daly, T. J., & Wu, C.-W. (1988) *J. Biol. Chem. 263*, 10272–10277.
Wolff, A. F., & Brown, D. D. (1988) *Science 241*, 1626–1632.
Wolff, A. F., Jordan, E., & Brown, D. D. (1986) *Cell 44*, 381–389.

A Novel Approach for Sequential Assignment of ^1H, ^{13}C, and ^{15}N Spectra of Larger Proteins: Heteronuclear Triple-Resonance Three-Dimensional NMR Spectroscopy. Application to Calmodulin†

Mitsuhiko Ikura, Lewis E. Kay, and Ad Bax*
Laboratory of Chemical Physics, NIDDK, National Institutes of Health, Bethesda, Maryland 20892
Received December 7, 1989; Revised Manuscript Received February 28, 1990

ABSTRACT: A novel approach is described for obtaining sequential assignment of the backbone ^1H, ^{13}C, and ^{15}N resonances of larger proteins. The approach is demonstrated for the protein calmodulin (16.7 kDa), uniformly (~95%) labeled with ^{15}N and ^{13}C. Sequential assignment of the backbone residues by standard methods was not possible because of the very narrow chemical shift distribution range of both NH and $C^\alpha H$ protons in this largely α-helical protein. We demonstrate that the combined use of four new types of heteronuclear 3D NMR spectra together with the previously described HOHAHA–HMQC 3D experiment [Marion, D., et al. (1989) *Biochemistry 28*, 6150–6156] can provide unambiguous sequential assignment of protein backbone resonances. Sequential connectivity is derived from one-bond J couplings and the procedure is therefore independent of the backbone conformation. All the new 3D NMR experiments use ^1H detection and rely on multiple-step magnetization transfers via well-resolved one-bond J couplings, offering high sensitivity and requiring a total of only 9 days for the recording of all five 3D spectra. Because the combination of 3D spectra offers at least two and often three independent pathways for determining sequential connectivity, the new assignment procedure is easily automated. Complete assignments are reported for the proton, carbon, and nitrogen backbone resonances of calmodulin, complexed with calcium.

Sequential resonance assignment of the backbone protons of a protein forms the basis for further solution structure studies by NMR.[1] This sequential assignment is most commonly accomplished by means of homonuclear ^1H 2D experiments that identify intraresidue through-bond $^3J(NH, H^\alpha)$ connectivity and sequential interresidue through-space (NOE) connectivity (Wüthrich, 1986; Kaptein et al., 1988; Clore & Gronenborn, 1989; Bax, 1989). Use of the interresidue NOE is essential in this approach because of the absence of a significant ^1H–^1H J coupling between protons of adjacent amino acids. This short-range interresidue NOE interaction depends strongly on the local conformation. In addition, many of these protons can also exhibit long-range NOE interactions, making unambiguous identification of sequential NOEs even more difficult.

In recent years, the sequential assignment procedure has been applied successfully to a large number of small proteins. For larger proteins (M_r > 10 kDa), or for proteins with a very narrow chemical shift distribution of the backbone proton resonances, the standard sequential assignment procedure may not yield unambiguous answers because of very extensive overlap in critical regions of the ^1H 2D NMR spectra. This overlap problem can be alleviated dramatically by the recording of isotope-edited 2D NMR experiments of proteins in which specific amino acids are isotopically labeled (McIntosh et al., 1987a,b; Senn et al., 1987; LeMaster & Richards, 1988; Fesik et al., 1988; Torchia et al. 1989). In a related double-labeling technique, one type of amino acid is labeled with ^{13}C in the carbonyl position and a second amino acid is labeled with ^{15}N. Any dipeptide fragment in which the amino acid labeled with ^{13}C precedes the ^{15}N-labeled residue can be easily identified on the basis of the $^1J_{CN}$ splitting

† This work was supported by the Intramural AIDS Antiviral Program of the Office of the Director of the National Institutes of Health. L.E.K. acknowledges financial support from the Medical Research Council of Canada and the Alberta Heritage Trust Foundation.

[1] Abbreviations: INEPT, insensitive nuclei enhanced by polarization transfer; HCACO, proton to α-carbon to carbonyl correlation; HCA(CO)N, proton to α-carbon (via carbonyl) to nitrogen correlation; HMQC, heteronuclear multiple quantum correlation; HNCO, amide proton to nitrogen to carbonyl correlation; HNCA, amide proton to nitrogen to α-carbon correlation; HOHAHA, homonuclear Hartmann–Hahn; NMR, nuclear magnetic resonance; NOE, nuclear Overhauser enhancement; 2D, two-dimensional; 3D, three-dimensional.